Available online at www.sciencedirect.com

SciVerse ScienceDirect

Procedia Engineering 48 (2012) 599 – 606

Procedia Engineering

www.elsevier.com/locate/procedia

MMaMS 2012

Modeling and Experimental Analysis of the Aluminium Alloy Fatigue Damage in the case of Bending – Torsion Loading

Milan Sága[a]*, Peter Kopas[a], Milan Uhríčík[a]

[a] *University of Žilina, Faculty of Mechanical Engineering, Department of Applied Mechanics, Univerzitná 1, 010 26 Žilina, Slovakia*

Abstract

The article deals with determining of fatigue lifetime of structural materials during by multiaxial cyclic loading. The theoretical part focuses on fatigue and criterions for evaluation of the multiaxial fatigue lifetime. The experimental part deals with modeling of combined bending - torsion loading and determining the number of cycles to fracture in region low-cycle fatigue and also during of the loading with the sinusoidal wave form under in phase $\varphi = 0°$. Based on the experimental results the fatigue design curves are compared to fatigue data from base metal and weldments.

Keywords: biaxial fatigue; low cycle fatigue; aluminum alloy; S-N curve; stress and strain; sinusoidal cyclic loading; TIG welding

Nomenclature

A	material parameter
b	fatigue strength exponent
b_γ	fatigue strength exponent in torsion
B	material parameter
c	fatigue ductility exponent
c_γ	fatigue ductility exponent in torsion
E	elasticity modulus in tension
f_f	factor of safety applicable the fatigue
G	elasticity modulus in torsion
k	material parameter
N_f	number of cycles to fracture
R_A	major axis of the ellipse
R_B	maximum distance of stress point
S	material parameter
S_e	modified fatigue strength
S_{ut}	ultimate tensile strength
Greek symbols	
α	material parameter

* Corresponding author.
E-mail address: milan.saga@fstroj.uniza.sk

1877-7058 © 2012 Published by Elsevier Ltd.Selection and/or peer-review under responsibility of the Branch Office of Slovak Metallurgical Society at Faculty of Metallurgy and Faculty of Mechanical Engineering, Technical University of Košice Open access under CC BY-NC-ND license.
doi:10.1016/j.proeng.2012.09.559

γ_f'	fatigue ductility coefficient in torsion
ε_f'	fatigue ductility coefficient
σ_f'	fatigue strength coefficient
σ_h^{mean}	mean hydrostatic stress
σ_n	normal stress
$\sigma_{n,max}$	maximum stress
$\sigma_{n,mean}$	mean stress
σ_y	stress in the direction of the axis y
τ_a	equivalent shear stress
τ_f'	fatigue strength coefficient in torsion
Δy_{max}	maximum shear strain range
$\Delta\varepsilon_1$	principal strain range
$\Delta\varepsilon_n$	normal strain range
$\Delta\tau/2$	alternating shear stress
$\Delta\tau_{oct}$	octahedral shear stress
ΔW	virtual strain energy

1. Introduction

Fatigue failure is an extremely complex physical process which is governed by a great number of parameters related to, for example, local geometry and material properties of the structural region surrounding the crack growth path. It is commonly recognized that it is impossible for a physical model to account for all fatigue influencing parameters, thus a lot of approximate models have been conceived for practical fatigue assessments. In every stadium of fatigue cumulative damage dominates a definite mechanism controlled by more or less known and verified rules. There exists the stage of micro-plastic process in total volume of material with following stage of fatigue crack nucleation and stage of their growing with more or less detailed zoning. Despite of this research no results have been achieved, which could be considered as successful ones. This applies mainly to the cases of random and combined stress, where today's procedures used in one axis stress analysis fails. There are different approaches and methods which can be used in fatigue life predictions [1, 2].

Fatigue under combined loading is a complex problem. A rational approach might be considered again for fatigue crack nucleation at the material surface [3]. The state of stress at the surface is two-dimensional because the third principal stress perpendicular to the material surface is zero. Another relatively simple combination of different loads is offered by an axle loaded under combined bending and torsion. This loading combination was tested in our and also in many others experiments [4-9]. In spite of this fact, fatigue mechanisms are still not fully understood. This is partly due to the complex geometrical shapes and also complex loadings of engineering components and structures which result in multiaxial cyclic stress-strain states rather than uniaxial.

1.1. Fatigue properties of the welded aluminum alloy

The strength analysis of welded structures does not deviate much from that for other types of structures. Various failure mechanisms have to be avoided through appropriate design, choice of material, and structural dimensions. Design criteria such as yielding, buckling, creep, corrosion, and fatigue must be carefully checked for specific loading conditions and environments. It is, however, a fact that welded joints are particularly vulnerable to fatigue damage when subjected to repetitive loading. Fatigue cracks may initiate and grow in the vicinity of the welds during service life even if the dynamic stresses are modest and well below the yield limit. The problem becomes very pronounced if the structure is optimized by the choice of high strength steel. The very reason for this choice is to allow for higher stresses and reduced dimensions, taking benefits of the high strength material with respect to the yield criterion. However, the fatigue strength of a welded joint is not primarily governed by the strength of the base material of the joining members; the governing parameters are mainly the global and local geometry of the joint. Hence, the yield stress is increased, but the fatigue strength does not improve significantly. This makes the fatigue criterion a major issue. The fatigue strength will alone give the requirements for the final dimensions of the structural members such as plates and stiffeners. To overlook this fact may result in fatigue facture and serious consequences [10, 11].

As already stated, the fatigue behavior of welded joints is random by nature. Very few load-bearing details exhibit such large scatter in fatigue life as welded joints. This is true even in controlled laboratory conditions. As a consequence, it becomes an important issue to take scatter into consideration, both for the fatigue process and for the final life. Furthermore, the in-services stresses may often be characterized as stochastic processes.

There has been a trend the last two decades to treat the strength problem of a structure by applying statistics and probability calculations. As a consequence, the probability of failure is used as a criterion, instead of the more traditional safety factors, when checking various design criteria. The methods and tools for performing this type of analysis have become available and quite easy to use. The probability of no failure during a given time period is considered to be the reliability of the structure. The methods used for determining the probability are often called reliability methods. Furthermore, if the associated probability of failure is weighed against the consequence of failure we arrive at the risk concept. Achieving high reliability and low risk levels will maintain operational capability and secure life and assets. The more sources of uncertainty there are in a structural problem, the more appropriate will be the application of a reliability approach. For processes where damage is accumulating with time, the probability of failure will increase with service time, depending on decisions made for the design concept, configurations, dimensions, material properties, and in-service inspection strategy.

For fatigue of welded joints the following sources of uncertainty are dominant [11-14]:

- the service stress history;
- the global and local geometry of the joint
- the material parameters
- the performance of the in-service inspection

1.2. Important topics for welded joints

The general issues described above are, of course, also important for welded joints. However, a welded joint has some peculiar features that make some of the subjects and parameters play a much more important role than others. Let us start with an S-N curve for a welded joint and compare it with other specimens. Figure 1 shows the S-N curves based on tests with one smooth plate, one plate with a bore hole, and one plate with a fillet welded transverse attachment (gusset). This type of fillet welded joint is often referred to as non-load-carrying due to the fact that the load is carried straight through the base plate. It is also noted that the applied force is transverse to the welding direction [10, 15-16]. In the plate, the fatigue cracks can appear anywhere in the longitudinal edges of the plate, whereas they will appear at the inner edges of the bore hole transverse to the applied loading in the specimen with the hole. The latter phenomenon is due to the stress concentration at the edge of the hole. In the fillet welded joint the cracks will appear at the weld toe and grow through the base plate in a direction perpendicular to the applied principal stresses. The cracks are indicated on the specimens in Fig. 1. The cracks may emanate from several spots along the weld seam. Small semi-elliptical-shaped cracks are formed, grow, and coalesce to become larger cracks. In the final stage the remaining ligament of the plate section is too small to carry the peak load. As can be seen from Fig. 1, the fatigue life for the fillet welded joint is significantly shorter than both the smooth plate and the plate with a bore hole [8-9].

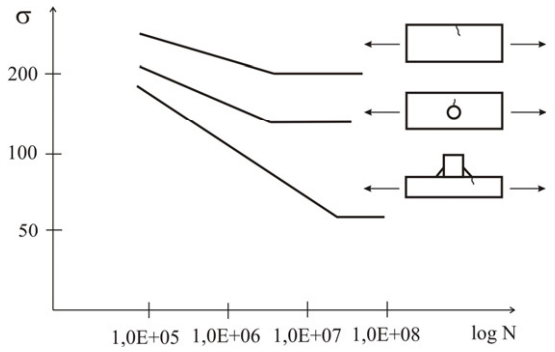

Fig. 1 Fatigue life curves for various details [8]

The difference between the S-N curve for the specimen with the hole and the S-N curve for the welded joint is rather surprising considering the fact that the bore hole creates a stress concentration factor close to 3 at the edge of the hole. The relatively short fatigue life of welded detail is explained, in the main, by three factors:

- severe notch effect due to the attachment and the weld filler metal
- presence of non-metallic intrusions or micro-flaws along the fusion line
- presence of large tensile residual stresses

1.3. Chosen criterions for multiaxial fatigue damage prediction

There are plenty of hypotheses used for evaluating a degree of damage caused by variable load [17,19,22]. Life prediction methods which presume homogeneous material (free from cracks, inclusions or defects) at the outset of the investigation can be divided into strain-based (low-cycle fatigue) and stress-based (high-cycle fatigue) methods. Low-cycle fatigue is characterized by repeated plastic strains during cyclic loading conditions where fatigue failure occurs after relative low number of load cycles (in the order of 10^4 cycles). This design approach is normally used in fatigue assessment of local areas where high stress concentrations exist and the material response locally is repeated plastic deformation. In addition, stress-based approaches use the elastic stress range (or amplitude) as the governing load parameter. At a sufficient load level, which may result in a fatigue life of approximately 10^7 cycles, a threshold referred to as the fatigue or endurance limit can be seen for many materials.

Research of mechanism and processes of fatigue failure of materials achieves great advance, however there still doesn't exist general failure model, which should be applicable for different conditions of activity. There is needed an integration for such a procedures into a modern systems of computing aided design (CAD) in relationship to methods of strength computing transferred by finite element method (FEM) [18, 20-22].

Criteria valid for the fatigue lifetime calculation can be classified in three different categories:

- strain based methods
- strain-stress based methods
- energy based approaches

Brown and Miller [22] observed that the fatigue life prediction could be performed by considering the strain components normal and tangential to the crack initiation plane. Moreover, the multiaxial fatigue damage depends on the crack growth direction. Different criteria are required if the crack grows on the component surface or inside the material. In the first case they proposed a relationship based on a combined use of a critical plane approach and a modified Manson-Coffin equation, where the critical plane is the one of maximum shear strain amplitude. Criterion which was created has the following form:

$$\frac{\Delta\gamma_{max}}{2} + S \times \Delta\varepsilon_n = A \times \frac{\sigma'_f - 2\sigma_{n,mean}}{E} \times \left(2 \times N_f\right)^b + B \times \varepsilon'_f \times \left(2 \times N_f\right)^c \quad . \tag{1}$$

Fatemi and Socie [23] observed that the Brown and Miller's idea could be successfully employed even by using the maximum stress normal to the critical plane, because the growth rate mainly depends on the stress component normal to the fatigue crack. Starting from this assumption, he proposed two different formulations according to the crack growth mechanism: when the crack propagation is mainly MODE I dominated, then the critical plane is the one that experiences the maximum normal stress amplitude and the fatigue lifetime can be calculated by means of the uniaxial Manson-Coffin curve; on the other hand, when the growth is mainly MODE II governed, the critical plane is that of maximum shear stress amplitude and the fatigue life can be estimated by using the torsion Manson-Coffin curve [22]. Criterion has the following form

$$\frac{\Delta\gamma}{2} \times \left(1 + k \times \frac{\sigma_{n,mean}}{\sigma_y}\right) = \frac{\tau'_f}{G} \times \left(2 \times N_f\right)^{b_\gamma} + \gamma'_f \times \left(2 \times N_f\right)^{c_\gamma} \quad . \tag{2}$$

Liu created a virtual model of the deformation energy, which is a generalization of the axial energy on the basis of prediction of fatigue life. Criterion has the following form:

$$\Delta W = 4 \times \sigma'_f \times \varepsilon'_f \times \left(2 \times N_f\right)^{b+c} + \frac{4 \times \sigma'^{\,2}_f}{E} \times \left(2 \times N_f\right)^{2b} \quad . \tag{3}$$

Smith, Watson and Topper (SWT) created a parameter for multiaxial load, which is based on the main deformation range $\Delta\varepsilon_1$ and maximum stress $\sigma_{n,max}$ to the main plane. Criterion has the following form:

$$\sigma_{n,mean} \times \frac{\Delta\varepsilon_1}{2} = \frac{\sigma'^{\,2}_f}{E} \times \left(2 \times N_f\right)^{2b} + \sigma'_f \times \varepsilon'_f \times \left(2 \times N_f\right)^{b+c} \quad . \tag{4}$$

2. Experimental material

This research was conducted on an AlMgSi07.F25 aluminum alloy: the EN AW 6063-T66 aluminum alloy. The EN AW 6063-T66 is a medium strength alloy, suitable for applications where no special strength properties are required. Simple to complex shapes can be produced with very good surface quality characteristics, and suitable for many coating operations

such as anodizing and powder coating. Typical areas of application for this alloy is architectural doors and windows, facades, furniture parts, lighting columns and flagpoles, heat sink sections, office equipment, trailer flooring, irrigation, heating and cooling pipes, ladders, railings. The T66 treatment corresponds to solution heat-treated and then artificially aged (precipitation hardened) to a higher level of mechanical properties through special control of manufacturing process. Such a heat treatment conditions make mechanical property level higher than T6 heat treatment conditions. The typical chemical composition of the EN AW 6063.T65 aluminum alloy is shown in Table 1. The high Magnesium content is responsible for the high corrosion resistance and good weldability. The proportions of Magnesium and Silicon available are favorable to the formation of Magnesium Silicide (Mg2Si). The material used in this research was delivered in the form of cylindrical shape with a diameter 10 mm. The length of cylindrical bars was 150 mm. The material was in rolled state.

Table 1. Chemical composition of the EN AW 6063-T66 aluminum alloy (weight %) according to EN 573-3

Si	Fe	Cu	Mn	Mg	Cr	Zn	Ti	Other		Al
								Each	Total	
0,20-0,60	0,35	0,10	0,10	0,45-0,90	0,10	0,10	0,10	0,05	0,15	rest

Figure 2 and Figure 3 illustrates a typical microstructure of the aluminum alloy evaluated in longitudinal and transversal direction. It is visible the stretched grains due to the rolling process. Also, a dispersed second phase typical of deformed and heat treated wrought aluminum alloys is observed.

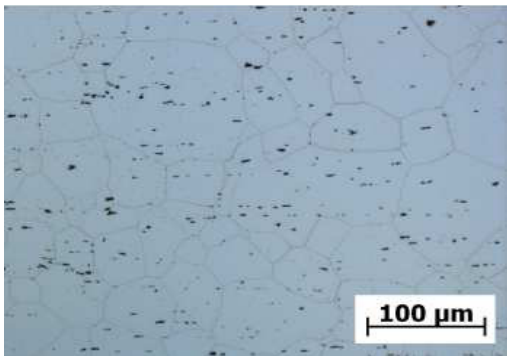

Fig. 2 Microstructure of the EN AW 6063.T66 aluminum alloy according the rolling direction, etch. 0,5% HF

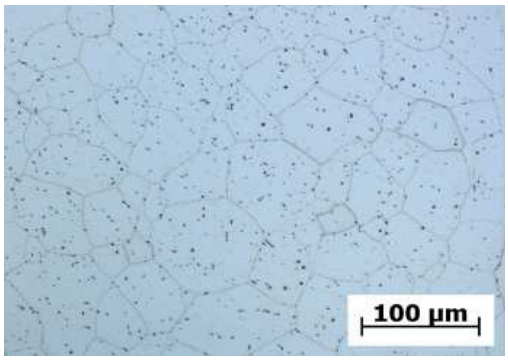

Fig. 3 Microstructure of the EN AW 6063.T66 aluminum alloy transversal the rolling direction, etch. 0,5% HF

Welding was conducted by the tungsten-inert gas (TIG) welding method using by Fronius Magic Wave 2200 welding machine. The welding factors used were: welding current I_z = 79 A; welding voltage U_z = 18,8 V; diameter of wolfram electrode Ø = 2,4 mm; welding gas Ar 99,996 % with gas flow Q = 15 $l.min^{-1}$. As a welding wire material there was used aluminum wire AlSi5 with diameter 2 mm. The joint strength of TIG-welded joints was evaluated by tensile testing and fatigue testing, using the test specimens shown in Fig. 4 and in Fig. 5. The hardness distribution of joints was measured along the axial center, at weld interface and at original material zone, using a Brinell hardness tester (HBW).

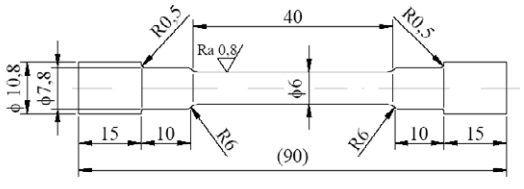

Fig. 4 Shape and dimension of tensile test specimen (dimension in mm)

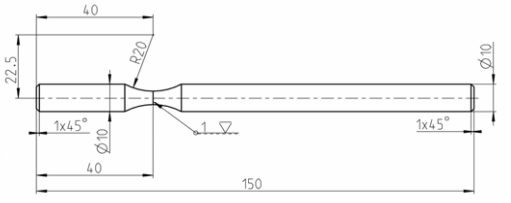

Fig. 5 Shape and dimension fatigue test specimen (dimension in mm)

Static tensile test with standard specimens realized before and after the welding process had also been carried out. Results are summarized in Tab. 2. The join geometry of the rod used for welding process is shown in Fig. 6. Figure 7 illustrate final shape of welded joint.

Table 2. Mechanical properties of the EN AW 6063.T66 aluminum alloy

Young modulus	62 500 MPa
Ultimate tensile strength	247 MPa
Tensile yield strength	212 MPa
Ultimate tensile strength of welded specimen	166 MPa
Tensile yield strength of welded specimen	79 MPa

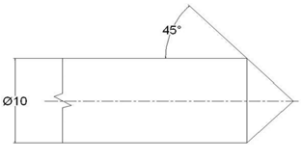

Fig. 6 Joint geometry (dimension in mm)

Fig. 7 Shape of welded joint

3. Experimental and numerical strain-life data results

Thirty smooth specimens were tested under strain controlled conditions in order to identify the strain-life behaviour of the experimental material. After machining, the specimen surfaces were mechanically polished. The experiments were carried out in an electro mechanic fatigue test machine, developed on University of Zilina. Design of experimental equipment has been based on mechanical principle. The constant rotation is generated by excenter and linkage mechanism. By changing of excentric magnitude it is possible to change a loading magnitude. Also if we change a length of connecting crank on the experimental equipment, there will be change in a loading cycle character. Power of device is secured by two synchronic electromotors with frequency converters from 0.5 Hz to 100 Hz. Loading frequencies are identical with frequency of rotation drive. Synchronization of the electromotors is secured using by electronics and allows synchronization of loading amplitudes. Synchronization of electromotors also allows setting phase shift for individual loading levels. There are also included two force measure systems in experimental equipment. These systems may be used for measurement of force values during the loading process. For evaluation of fatigue curves it needs to know stress and strain conditions on individual loading levels. A sinusoidal waveform was used as command signal. The fatigue tests were conducted with constant strain amplitudes, at room temperature, in air. The specimens were cyclic loaded under strain control with symmetrical proportional bending-torsion loading, with a nominal strain ratio, $R_\varepsilon = -1$. The computational fatigue tests were performed under in-phase cyclic loading with the zero mean value. All tests were performed under controlled bending and torsion moments. Frequency of each analysis was equal to 30 Hz.

The results, fatigue resistance (strain amplitude vs. number of cycles to failure) of tested structural material EN AW 6063.T66 before and also after welding process (TIG) in the low cycle regime are presented in Fig. 8 and Fig. 9. In the low cycle regime of loading the strain amplitude decreases with increasing of cycles number to failure for both series of aluminum alloy.

The first series of performed experiments (without welding joint) were to verify fatigue behavior low-cycle bending and low-cycle torsion loading to obtain relation between strain magnitudes versus number of cycles to failure. The second series of performed experiments (with welding joint) were to also verify fatigue behavior of aluminum alloy EN AW 6063.T66 under low-cycle bending and torsion loading to obtain relation between strain magnitudes versus number of cycles to failure. The Fig. 8 had shown the results of fatigue tests with the symmetrical pure bending loading for base material in comparison with welded joints. The specimen failure criterion during the testing was a creation of fracture area more than 90% in the measured cross section of the testing rod for both series.

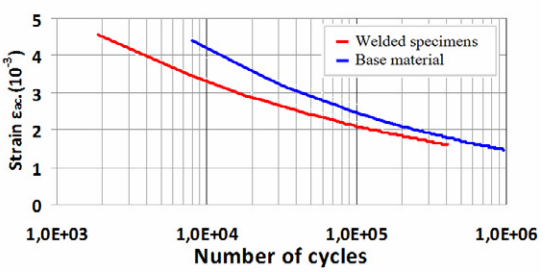

Fig. 8 Manson-Coffin curves for uniaxial low-cycle bending fatigue with phase shift 0°

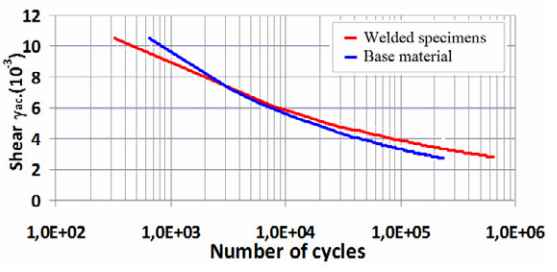

Fig. 9 Manson-Coffin curves for uniaxial low-cycle torsion fatigue with phase shift 0°

In ANSYS software was created the model of the test bar. The real geometry of this component is shown in Fig. 5. The rod bar had a circular shape with a defined section, in which was expected an increased concentration of stress and creation a fatigue fracture. The ends of this model were loaded by reversed bending moment on the one side and by reversed torsion moment on the opposite site. The values of presented stresses and strains in the middle of the rod radius were taken from computational analysis using finite element method. We used the same material parameters in finite element model as are shown in Tab. 2.

Obtained values of the stresses from finite element analysis were next computational analyzed using Fatigue Calculator software. This is a program which can quickly calculate fatigue lifetime of selected material. After starting the calculation, Fatigue Calculator displayed the number of cycles to failure for different models of damage. In our calculation we considered with all multiaxial criteria described above which can be applied to low-cycle fatigue region. The computational fatigue tests were performed under in-phase cyclic loading with the zero mean value. All the tests were performed under controlled bending and torsion moments. Frequency of each analysis was equal to 30 Hz. The results, fatigue durability of EN AW 6063.T66 with different models of damage (stress amplitude vs. number of cycles to failure) in the low-cycle regime are presented in Fig. 11. The obtained results can be discussed i.e. from the point of view of multiaxial criteria applied on low-cycle region of fatigue loading. Generally, we can say, that stress amplitude continually decreasing with number of cycles to failure increasing after conventional limit of cycles number (N_C = 2.10^6 cycles to N_C = 1.10^7 cycles) used to fatigue limit σ_C determination.

From computational analysis can be seen that the area with greatest concentration of stresses or eventually the place with the higher deformation was localized in the middle of the rod radius (see Fig. 10).

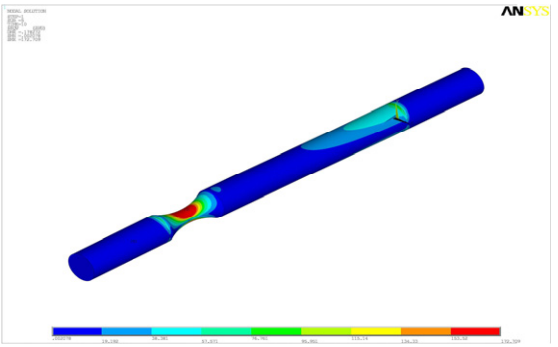

Fig.10 Result of FEM analysis

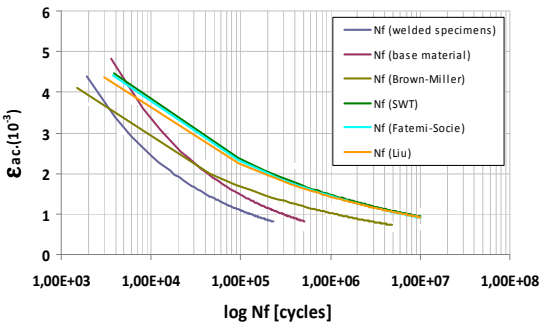

Fig.11 Manson/Coffin curves for multiaxial low-cycle fatigue with phase shift 0°

4. Conclusion

Generally we can say that results are in good agreement with published results of other authors [10-14]. The differences in fatigue resistance of aluminum alloy both series of specimens are caused by different type of loading. Fatigue under cyclic bending are not that much different in comparison during by torsion loading. Fatigue strength of the welded specimens decreased for bending and torsion cyclic loading compared to that of the base material, EN AW 6063.T66. The decrease in fatigue strength of the welded specimens was attributed to the stress concentration at the toe of weld.

Residual stresses are an important factor influencing the structural behavior in all instability failures as well as in fatigue crack initiation and propagation when cyclic service stresses are superposed onto the residual stresses. It is generally and conservatively assumed in design that tensile residual stresses up to the proof strength of the material will be present in a welded structure. The existence of tensile residual stresses in a surface layer accelerates crack initiation reducing fatigue life due to the increase of local mean stress. An improvement in the fatigue life of the welded joints can be related to the fact that generally the T66 heat treatment produces an almost completely relief of tensile residual stresses in Al-alloy weldments. Therefore the slope of fatigue curves in Fig. 8 and Fig. 9 are similar.

All multiaxial models applied to fatigue lifetime calculation of aluminum alloy EN AW 6063.T66 increases with decreasing stress amplitude continuously in the cycles of number region. Considering the low-cycle region the fatigue curves have shown a good agreement of progress line with Fatemi-Socie, SWT and Liu damage models. For Brown-Miller model it was also observed significant decrease of stress amplitude with increasing number of cycles to failure but the fatigue endurance values in comparison with reference number of cycles were markedly lower as for Fatemi-Socie, SWT and Liu damage multiaxial models.

Acknowledgements

This work has been supported by VEGA grants No. 1/1089/11 and No. 1/0125/09. The authors gratefully acknowledge this support.

References

[1] Balda, M., Svoboda, J., Fröhlich, V., 2003. *Using hypotheses for calculating fatigue lives of parts exposed to combined random loads*, Engineering Mechanics, Volume 10, Issues 5, p. 12-15.

[2] Carpinteri, A., Spagnoli, A., Vantadori, S., 2003. *A multiaxial fatigue criterion for random loading*, Special Issue of Fatigue and Fracture of Engineering Materials and Structures, Vol. 26, No. 6, p. 515-522.

[3] Nový, F., Kopas, P., Bokůvka, O., CHalupová, M., 2003. *Vplyv zlievarenských chýb na únavovú životnosť perliticko – feritickej LGG*. Materiálové inžinierstvo, 3, 10, SK.

[4] Bigoš, P., Trebuňa, F.: *Metodicke postupy riešenia otazok zostatkovej životnosti nosnych konštrukcii experimentalnymi metodami*. Acta Mechanica Slovaca 2/98. Košice 1998. ISSN 1335-2393.

[5] Trebuňa, F., Buršak, M.: Medzne stavy, lomy. Grafotlač, Prešov 2002. ISBN 807165-362-4.

[6] Bannantine, J. A., Socie, D. F., 1992. *A multiaxial fatigue life estimation technique.* In: Advances in Fatigue Lifetime Predictive Techniques, ASTM STP 1122. Eds: M. R. Mitchell a R. W. Landgraf. Philadelphia, American Society for Testing and Materials, pp. 249-275.

[7] Leger, J., 1989. *Fatigue life testing of crane drive shafts under crane-typical torsional and rotary bending loads*. Schenck Hydropuls Mag., Issue 1/89, pp. 8–11.

[8] Gough, H.J., Pollard, H.V., 1935. *The strength of metals under combined alternating stresses.* Proc. Inst. Mech. Engrs, Vol. 131, pp. 3–103.

[9] Gough, H.J., Pollard, H.V., 1951. *Some experiments of the resistance of metals to fatigue under combined stresses.* Min. of Supply, Aero Res. Council, RSM 2522, Part I.

[10] Maddox, S. J., 1991. *Fatigue strength of welded structures*, Second Edition, Woodhead Publishing, UK, ISBN 978-1855730137.

[11] Mathers, G., 2002. *The welding of aluminium and its alloys*. Published by Woodhead Publishing Limited, Abington Hall, Abington Cambridge CB1 6AH, England, ISBN 0-8493-1551-4.

[12] Borrego, L.P., Abreu, L.M.; Costa, J.M., Ferreira, J.M., 2004. *Analysis of Low Cycle Fatigue in AlMgSi Aluminium Alloys.* Engineering Failure Analysis, Vol. 11, pp. 715-725.

[13] Chung, Y.S., Abel, A., . *Low Cycle Fatigue of Some Aluminum Alloys.* In: Low Cycle Fatigue, ASTM STP 942, H., American Society for Testing and Materials, Philadelphia, PA, pp. 94-106.

[14] Irving, B., 1994. *Welding the four most popular aluminum alloys.* Weld. J., 73 (2), pp. 51-55.

[15] Lassen, T., Récho, N., 2006. *Fatigue Life Analyses of Welded Structures.* ISTE Ltd, ISBN 978-1-905209-54-5.

[16] Chu, C., 1997. *Multiaxial fatigue life prediction methods in the ground vehicle industry.* Int J Fatigue, Vol. 19, Suppl. 1, pp. 325-330.

[17] Vaško, A., Vaško, M., 2010. *Microstructure and Mechanical Properties of ADI in Dependence of Transformation Temperature*, *Chapter 9*. In Process Inovation. Dnipropetrovsk : Yurii V. Makovetsky, 2010, p. 112–119.

[18] Langlais, T., 1999. *Computational methods for multiaxial fatigue analysis.* (Ph.D. Dissertation, University of Minnesota).

[19] Sága, M., 2004. *Mass Minimising of Truss Structures Subjected to Prescribed Fatigue Life.* Machine Dynamics Problems, Vol. 28, No. 4, pp. 101-106.

[22] Segľa, Š., 2007. *Dynamic and quasistatic analysis of the elevating work platform*. Journal Mechanisms and Manipulators, Vol. 6, Nr.1, pp. 81-86.

[21] Socie, D.F., 1987. *Multiaxial fatigue damage models.* J Eng Mater Technol, 1069, p. 293-298.

[22] Brown, M. W., Miller, K. J., 1973. *A theory for fatigue under multiaxial stress-strain conditions.* In: Proc. Inst. Mech. Engrs, Vol. 187, pp. 745-755.

[23] Fatemi, A. , Socie, D. F., 1988. *A critical plane approach to multiaxial fatigue damage including out-of-phase loading.* Fatigue Fract. Engng. Mater. Struct. 11 3, pp. 149-166.